Pure appl. geophys. 161 (2004) 1561–1578
0033 – 4553/04/071561 – 18
DOI 10.1007/s00024-004-2521-6

Pure and Applied Geophysics

Results of Analysis of the Data of Microseismic Survey at Lanzarote Island, Canary, Spain

A. V. GORBATIKOV[1], A. V. KALININA[1], V. A. VOLKOV[1], J. ARNOSO[2], R. VIEIRA[2], and E. VELEZ[2]

Abstract — From the data of a microseismic survey of the Lanzarote Island territory (Canary Archipelago) we obtained a microseisms amplitude distribution in the frequency range 0.3–12.5 Hz. We found a distinguished anomaly such as an amplitude depression, whose size and magnitude depend on the frequency. After studying the statistical and polarization properties of microseism signals we proposed a model explaining this depression, based on the presence of a rigid intrusive body in the center of the island. Results of our survey coincided well with independent detailed gravity survey results whose interpretation also implies the presence of intrusion. We estimated shear-wave velocity for the rocks of intrusion and for surrounding rocks using microseismic data.

Key words: Microseisms, survey, amplitude anomaly, intrusion, Lanzarote, Canary.

1. Introduction

Using microseisms – the Earth's surface weak background oscillations – to gain information regarding peculiarities in the structure and mechanical parameters of subsurface zones is very attractive. First, microseism signals are always present at any point on the Earth's surface. Second, the measurements themselves both in the methodical and expense aspect are much easier, as a rule, compared to other seismological methods. That is why many authors developed the methods utilizing microseisms as a sounding signal. More or less established terminology has appeared in this area. The distribution between long-period (T > 1 s) and short-period (T < 1 s) corresponds to the traditional distinction between "microseisms" with natural origin and "microtremors" with artificial origin (BARD, 1999). Microseisms are widely used for site response effect studies. It is recognized as an important factor to be considered in seismic microzonation.

[1] Joint Institute of Physics of the Earth, Russian Academy of Sciences, B. Gruzinskaya, 10, Moscow 123995, Russia. E-mails: avgor70@mail.ru; kalinina@uipe-ras.scgis.ru; volkov@uipe-ras.scgis.ru

[2] Instituto de Astronomía y Geodesia (CSIC-UCM), Universidad Complutense de Madrid, Facultad de Matemticas, 28040 Madrid, Spain. E-mails: vieira@iagmat1.mat.ucm.es; arnoso@iagmat1.mat.ucm.es; emilio_velez@mat.ucm.es

Microseisms research began as far back as the early works of OMORI (1908) and was developed both by the study of the microseism sources nature and their applications for local site response problems and engineering purposes. Concerning the microseisms origin, we know already since GUTENBERG (1927) that they appear as a result of atmospheric perturbations transmission for the waters of oceans and propagate over continental surface as Love and Rayleigh type waves. A high efficiency of their propagation is explained by their surface nature.

Many authors studied the microseisms nature. For example, AKI (1957); LACOSS *et al.* (1969), OMOTE and NAKAJIMA (1973), ASTEN, (1978), IRIKURA and KAWANAKA, (1980), SATO *et al.* (1991), HOUGH *et al.*, (1992), GORBATIKOV and BARABANOV (1994) studied the structure of short-period microseisms, their connection with geological structure and its condition, using seismic arrays and separate instruments. SAKAJIRI (1982); HORIKE (1985) on the other hand investigated the nature of long-period microseisms and their connection with the subsurface structure.

A solid majority of papers devoted to microseisms utilization, could be classified into three groups by their methodical approaches. This classification was suggested by LERMO and CHAVEZ-GARCIA (1994). The first group implies direct interpretation of Fourier spectra (e.g., KANAI and TANAKA, 1954; KATZ and BELLON, 1978); the second one – calculation and study of spectral relations between reference and studied site (e.g., OHTA *et al.*, 1978; KAGAMI et al., 1986; FIELD *et al.*, 1990); the third group includes determination of spectra relations between horizontal and vertical spatial components (NAKAMURA, 1989).

We use microseisms as a sounding signal in our study as well. In contrast to the majority of researchers studying the properties and response of sediment layer lying on some rigid basement, the specificity of our subject is that we are interested in a further degree to know the properties of the basement in comparison to the sediments. This paper could be referred to as the second group of the adduced classification in a methodical aspect. We study the spatial distribution of spectral amplitudes of microseisms ranging 0.3–12.5 Hz.

Customarily researchers look for additional information for the verification of the results of microseismic study when microseisms are used for microzonation. In one case (UDWADIA and TRIFUNAC, 1973; CHAVEZ-GARCIA *et al.*, 1995) a zonation map was either confirmed with real accelerograms of a strong earthquake, or with the map of intensities built on results of the investigation. In a different case (MATSUSHIMA and OKADA, 1990) the microseismic zonation map found its confirmation in drilling data along some profile with subsequent verifying calculated evaluations.

In our paper we use independently obtained detailed gravity survey data as comparative information (CAMACHO *et al.*, 2000), and endeavor to make a complex interpretation of these two fields.

2. Geophysical Observations at Lanzarote Island

The Lanzarote Island belongs to the Canary Archipelago which is located at the edge of the West African Continental Margin. The island has an elongated shape and is situated at the northeast side of the archipelago. Its orientation has a SW-NE direction. It is approximately 55 km in length and 20 km in width. Lanzarote is defined by a shallow basement, probably about 4–5-km thick as deduced from seismic profiles (BANDA *et al.*, 1981). The basement is formed by a group of sedimentary rocks (quartzite and shale), plutonic rocks (basic and ultra-basic), and sub-volcanic rocks (basaltic and rachitic dikes) with an abundance of xenoliths of quartzite and sandstone emitted by its volcanoes. A solid majority of earlier geophysical research deals with extended surrounding oceanic areas and islands. We concentrate our study on the Lanzarote Island only and aim at revealing the peculiarities concerning its upper crust.

We should note here that the Institute of Astronomy and Geodesy of Madrid University has long conducted stationary observations at the underground geodynamic observatory, placed in the lava tunnel Cueva de los Verdes at the northeast edge of the island. The observatory is equipped with a number of instruments for observing the gravity field tidal variations, mareographs, meteorological instruments and others. On the west side of the island in Timanfaya National Park a measurement of microseismicity is being conducted as well as a measurement of heat flow and gas analysis (VIEIRA, 1991; ARNOSO, 2001). Since 1995 a tiltmeter station based on Ostrovsky pendulums and seismic station has been installed in frames of cooperation between Madrid University and the Institute of Physics of the Earth, Russian Academy of Sciences.

3. Microseisms Observations

Developing seismic observations on the island is of great interest, especially concerning registration of the local weak seismicity for its comparison with geodynamic processes. It was the challenge of searching for the appropriate places for future long-term regional seismic stations which iniated the plan for a microseism survey.

We conducted observations during two cycles – in summer 2000 and in summer 2001. The second cycle had a specifying character and was organized based on results of the first one. For the first cycle we chose 30 observational sites which were regularly distributed along the island territory (if the opportunity was offered). One of the sites was organized in the tunnel 18 deep from the day surface. During the second cycle we conducted measurements not along the surface but along a definite profile crossing an anomalous zone revealed during the first cycle. The profile

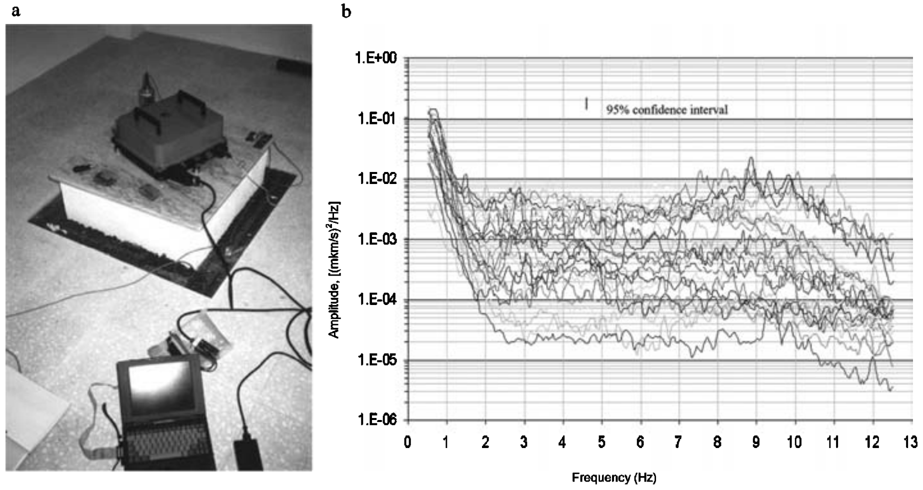

Figure 1

(a) Seismometer and acquisitioning system used in microseismic survey. (b) All measured (64 times stacked) spectra obtained at Lanzarote during microseismic survey, summer 2000 campaign.

contained 10 measurement sites. Figure 4 shows the locations of sites in the first cycle and Figure 5a shows the sites in the second cycle profile.

For observations we applied a movable station with control from a book-type computer, with power supply from an accumulator battery and with one 3-component seismometer. Our registering system provided 3 channels of velocimeter type with a frequency band 0.3–12.5 Hz, maximum sensitivity 80000 Volt*sec/meter with the possibility of gradual attenuation. The ADC had a resolution of 16 bits and the sampling rate was 100 samples per second by channel (see Fig. 1a).

Examples of fragments of microseisms are presented in Fig. 2a. The figure demonstrates the possibility of visually evaluating amplitudes and the character of microseisms on the island. We can see that a low frequency component with character periods of about 1 second prevails in the signal. The amplitude of those oscillations in displacements achieves 1 micron, which is an enormous value. For high frequencies beginning from 2 Hz, amplitudes by visual estimations achieve 0.1–0.01 microns. Such amplitudes are not unusual but typical for many places on the Earth.

During the survey we measured microseismic signal power spectra and stacked them 64 times at each site. For individual power spectra we used signal fragments of 20 seconds, with their preliminary multiplying by a Hunning window. We will discuss

Figure 2

(a) Fragment of microseisms signal at Lanzarote both in displacement and velocity. (b) Examples of particle motion projections obtained at site 14. The projections are given in relative units.

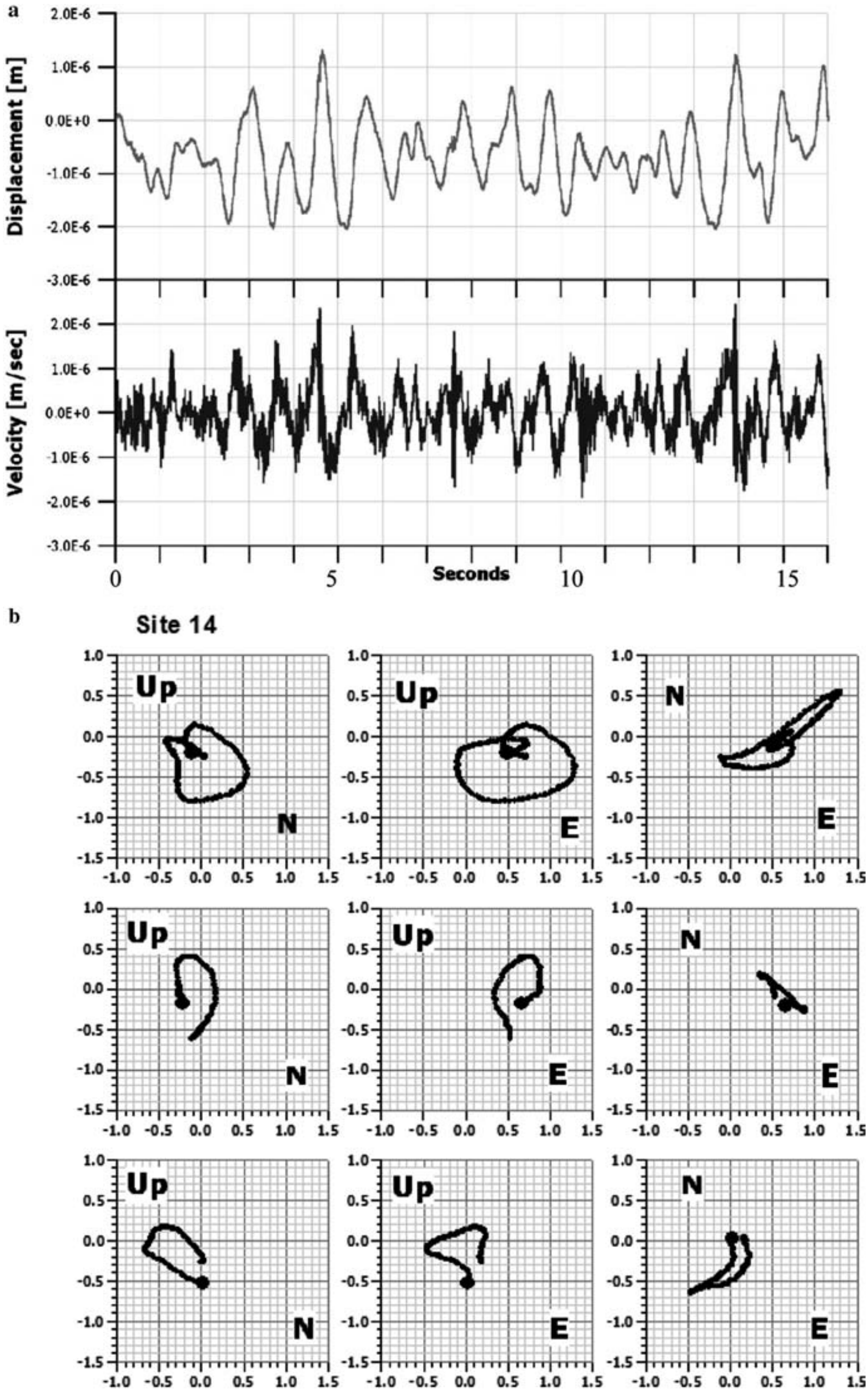
a
Displacement [m]
Velocity [m/sec]
Seconds
b
Site 14
Up
N
E

later a question concerning the number of stacking ($N = 64$) chosen as optimum. We registered microseisms with three reciprocal components; however for further processing we took only vertical component records to date. Thus, all the following speculations in this paper will concern the vertical component data only.

Figure 1b shows all measured stacked power spectra. A significant difference between individual spectra attracts the attention. The difference between spectral amplitudes achieves a magnitude of two orders in the frequency band 2–12 Hz. Regarding the low frequency part, considerable variations in amplitudes could be seen here as well. It is interesting to see that spectra exist with high low-frequency and low high-frequency components, however, one can find spectra with the inverse behavior. To provide correct interpretation of the observations it is important to answer two essential questions: 1. To what degree are the differences between the measured spectra significant? Or in other words, are the microseisms signal stationary and in which interval. After answering the question we would be able to compare the spatially separated sites where measurements were done asynchronously. 2. What type of waves compose the microseismic signal on the island in main? This aspect will be important when we evaluate the medium based on the received data.

4. Signal Properties Study

We conducted two special experiments in order to evaluate the stationary properties. In the first experiment we installed the microseismic station in one of the network sites for a period slightly exceeding one day (26 hours). Similar to all the other sites of the network, the measurement consisted of 64 times power spectra stacking, but was periodically repeated in the 26-hour period of the experiment. The resulting stacked spectra are exhibited as a surface on Figure 3b. Here the vertical axis is marked in logarithms of spectral amplitudes, the X-axis means frequency and the Y-axis means time marked from right to the left. We can see from the figure that the experiment started on 31.05.2001 at 20:09 local time and concluded late evening the next day. A night period can be well distinguished on the surface. Amplitudes smoothly decrease nearly ten times less from about 3–4 a.m. and then rather sharply increase from 8–9 a.m. However these variations do not concern the entire spectra but only frequencies ranging higher than 1.5 Hz. The lower frequencies are not exposed to this daily influence. We can see this from the behavior of isoline parallel to X-axis at frequencies lower than 1.5 Hz. In fact the applied approach is reminiscent of those

▶

Figure 3

(a) Illustration for the stationarity properties study. The examples of standard deviation behaviour in increasing time window are presented for four chosen sites. (b) The 64 times stacked spectrum behaviour in time during a one-day period.

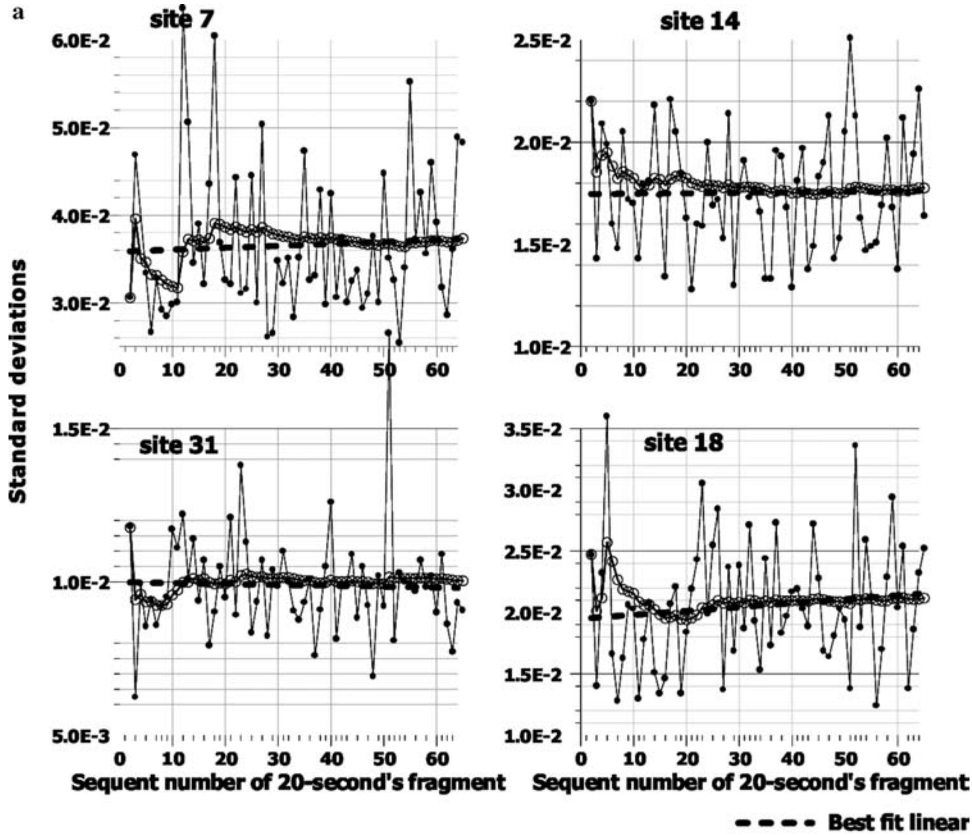
a
site 7
site 14
site 31
site 18
Standard deviations
6.0E-2
5.0E-2
4.0E-2
3.0E-2
2.5E-2
2.0E-2
1.5E-2
1.0E-2
3.5E-2
3.0E-2
5.0E-3
0 10 20 30 40 50 60
Sequent number of 20-second's fragment
Sequent number of 20-second's fragment
Best fit linear

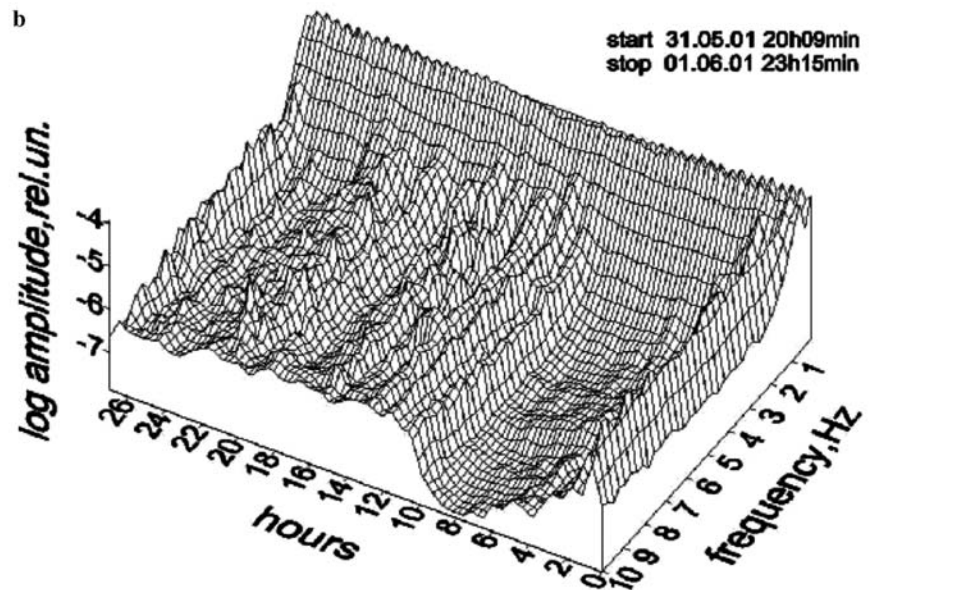
b
start 31.05.01 20h09min
stop 01.06.01 23h15min
log amplitude,rel.un.
-4
-5
-6
-7
26 24 22 20 18 16 14 12 10 8 6 4 2 0
hours
10 9 8 7 6 5 4 3 2 1
frequency,Hz

proposed by Seo *et al.* (1996) for distinguishing microseisms from microtremors where significant daily amplitude variations clearly indicate microtremors.

One more analogous experiment was conducted at another site. We measured a stacked power spectrum at one and the same place but in days with different weather conditions. We purposely chose a windy day and a day with very calm weather. The result was similar to the previous one. Wind influence occurred only on frequencies higher than 1.5 Hz. Thus we can preliminarily conclude that for frequencies lower than 1.5 Hz we can make asynchronous measurements and compare separated in space sites with each other.

The question about stationarity concerned the observational period optimization. We had to determine the optimal number of stacking while measuring the power spectrum at each site. Assuming from previous data that the microseism signal is a random Gaussian process with its mean value equal to zero, we could consider applicable the following relation between dispersion and spectral density:

$$\sigma_x^2 = 2\int_0^{\infty} S_x(f)df \quad , \tag{1}$$

where $x(t)$ is a random microseismic process, ${\sigma_x}^2$ and $S_x\,(f)$ is its dispersion and spectral density, correspondingly (Bendat and Piersol, 1966).

Taking into account (1), let us consider the behavior of dispersions of microseisms amplitude measured at four different sites (Fig. 3a). On all figures the values of standard deviations are laid along the Y-axis. The large dots indicate standard deviations defined on twenty-second fragments of the record. The empty circles indicate standard deviations in a window with increasing size, which is divisible by the twenty-second interval. A number of twenty-second intervals are laid along the X-axis, and they in turn constitute one long interval. We can well see that the standard deviations remain more or less equal from the beginning to the end of the experiment within each twenty-second interval. However a standard deviation in increasing window comes to a certain stable value after several oscillations at the beginning. The best-fit lines built on the clouds of short interval standard deviations are shown by dashes. We see that for all four exhibited cases the standard deviation in the increased window coincides with the best fit line after the long window length increases up to about 40 short intervals. The deflection does not exceed 3%. From this figure and relation (1) we can conclude that after 40 times stacking already the microseisms spectrum becomes stationary. For the microseismic survey itself we took 64 as a number of stacking. It exceeds with a 30% reserve the experimentally defined boundary and is convenient for a number of technological reasons.

The solution question regarding a content of microseisms at Lanzarote leads towards two illustrations following below. Figure 2b contains examples of three projections for 3-D particle oscillating motion in microseisms. In the presented cases projections on the vertical planes have a view of ellipsoids, and projections on horizontal plane have a linear form. Here the beginning of the oscillation phase is indicated with a large dot. We can trace the motion direction in the oscillation. We see that the oscillation character corresponds to the motion in the Rayleigh-type surface waves. From these examples we can also estimate a direction to the source. The projections on horizontal plane make it possible to perceive that the source for the given oscillating phases is not the only one. We analyzed many more examples than presented here. But due to size limitation of this paper we do not illustrate all the cases. From our analysis we saw that there is no singled out source of the microseisms on the island. The source looks like a distributed one. This is not surprising considering that the island has limited sizes and its shores are permanently subjected to the ocean surf impact. We also concluded that microseisms' energy is defined mainly by the contribution of Rayleigh-type waves.

To verify this we conducted an independent experiment which consisted in comparatively of the microseisms amplitude at frequencies 0.5–1.5 Hz measured both at a site on the day surface and on the depth 18 meters beneath the chosen point. We used a fortunate circumstance for our measurements – the presence of a natural lava tunnel, and found an attenuation of signal with the depth. The attenuation was frequency-dependent and increased in magnitude the higher the frequency was. Besides the amplitude, dependence on the frequency coincided with that calculated for the Rayleigh wave, under the assumption of shear-wave, velocity at that point had a value $V_S \cong 100$–200 m/s. Thus we obtained indirect proof that microseisms ranging from 0.5–1.5 Hz are presented with surface waves of Rayleigh type. Resultingly Figure 1b shows that the main part of energy originates from the frequency range 0.5–1.5 Hz and we can conclude that microseisms are mainly presented with Rayleigh waves.

5. Results of Observations

The results of our observations are shown in two figures – Figure 4 and Figure 5b. Figure 4 illustrates the first cycle observation results. Figure 5b contains results of the second cycle. Figure 4 has six sheets, with each corresponding to some frequency indicated at the top-left corner of the sheet. Each sheet represents a surface of experimental amplitude's distributions. Amplitudes in turn were selected from the row of the stacked spectra in Figure 1b. All sheets contain the island contour and observational sites are indicated with empty triangles. It is necessary to mention that average amplitudes for the different frequencies in spectra differ (Fig. 1b). Thus, to achieve maximum contrast we normalized the surface images independently – each to its own amplitude. We observe that an area with depressed amplitude values can be distinguished. This area located in the central part of the island and is slightly shifted to its east coast. The nearest settlement to the zone is named San-Bartolome.

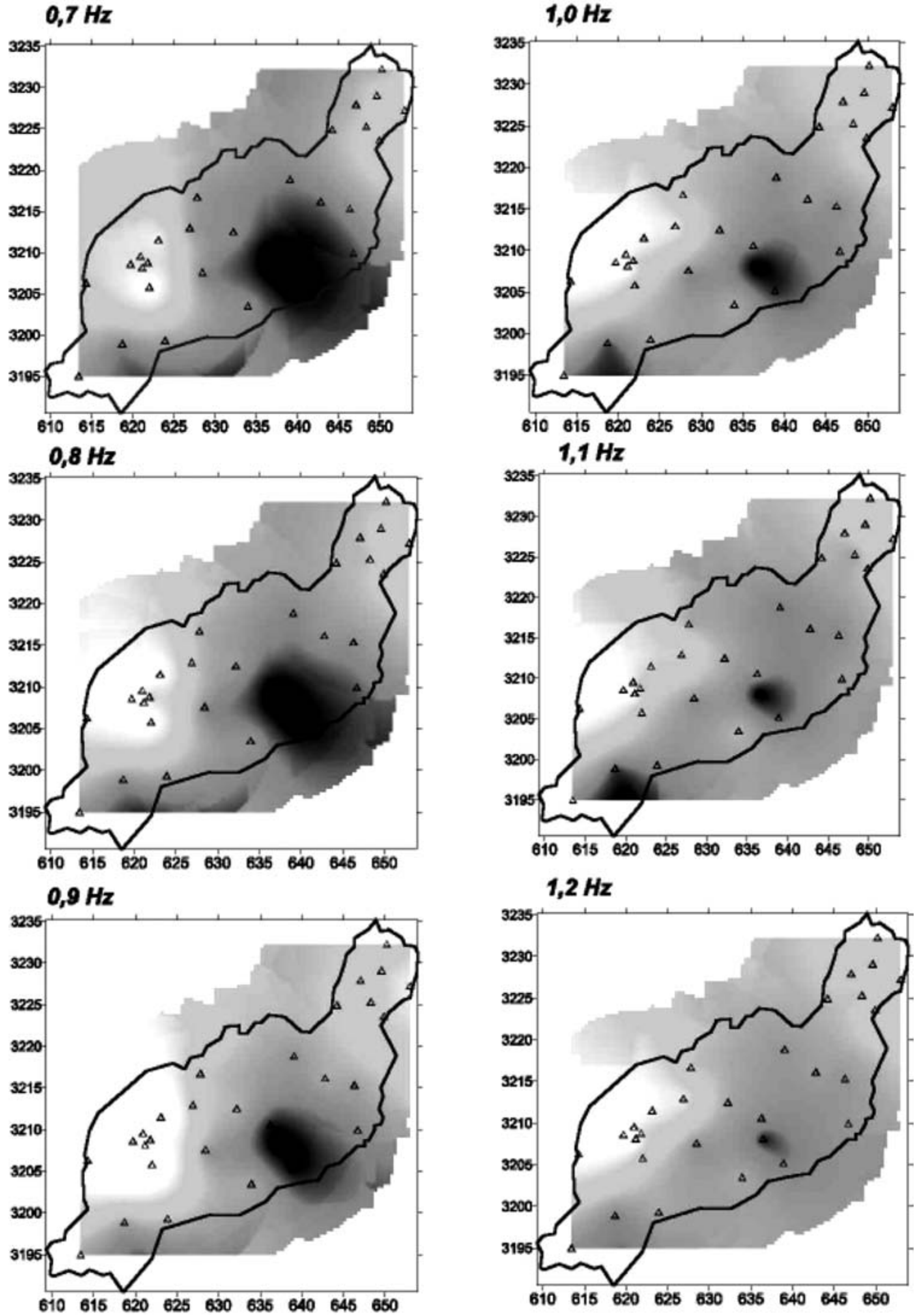
0,7 Hz
1,0 Hz
0,8 Hz
1,1 Hz
0,9 Hz
1,2 Hz
3235
3230
3225
3220
3215
3210
3205
3200
3195
610 615 620 625 630 635 640 645 650

The size of this area and the depth of the depression depend on frequency. Figure 4 contains surfaces for the frequencies from 0.7 Hz onwards. We do not adduce here the lower frequencies, as they do not differ considerably from the 0.7 Hz sheet. The depressed amplitude area decreases in size and concentrates around a certain point when the frequency increases from 0.7 to 1.2 Hz. From 1.3 Hz on this area mostly cannot be seen on the background.

We assume that this dependence can be explained only under the assumption that microseisms are present with the surface–type waves. Furthermore, it is necessary to assume the presence of geological inclusion more rigid by its mechanical properties than surrounding rocks. It is necessary to presume also that this inclusion does not appear at the surface, but rather is hidden under a certain sediment layer where the amplitude depression is disappearing beginning from the frequency 1.3 Hz. Under those assumptions the depression forming looks like the following. A surface Rayleigh wave propagates across the island and if it has enough length and thus enough deep penetration to the depth, it runs against the rigid inclusion. When propagating across the inclusion the wave amplitude decreases. If the wavelength is not long enough and penetration is not deep then the wave does not touch the inclusion and pass above it.

The fact of stable amplitude loss at a definite area is interesting because microseisms amplitude growth can be observed in practice very often. Besides, one can find numerous reasons for amplitudes growth than for the loss. It could be the influence of cultural sources for example.

We decided to verify this result again, and as we stated before, during next field season we conducted an additional cycle of microseismic survey. This survey consisted of the observations along the profile. Figure 5a shows the distribution of the observational sites relative to the island contour and the revealed zone of anomalous amplitudes depression. Observational results are presented in Figure 5b as dependence of microseisms' amplitudes (indicated by inking) both on the frequency (along the vertical axis) and on the coordinate in the profile (along the horizontal axis). The observational sites were placed imprecisely along a straight line and thus Figure 5b relates to a conditional line indicated on the figure by dashes.

We observe that the first cycle results are being proved. As in the first case we find the depression above the revealed zone at frequencies 0.5–0.8 Hz. As in the first case we found the depression size and depth decrease with the frequency growth. Starting from the approximate frequency 1.25 Hz, this depression is no longer noticeable on the background. Additionally we see on Figure 5b that with frequency growth from 1.3 Hz, the amplitude distribution character in the profile changes to the opposite

◀

Figure 4
Amplitude distribution of indicated frequency components along the territory of the island. The inking of each pattern is normalized by the average amplitude of the indicated frequency in the experimental spectra. Empty triangles show the places of the survey network for the summer 2000 campaign.

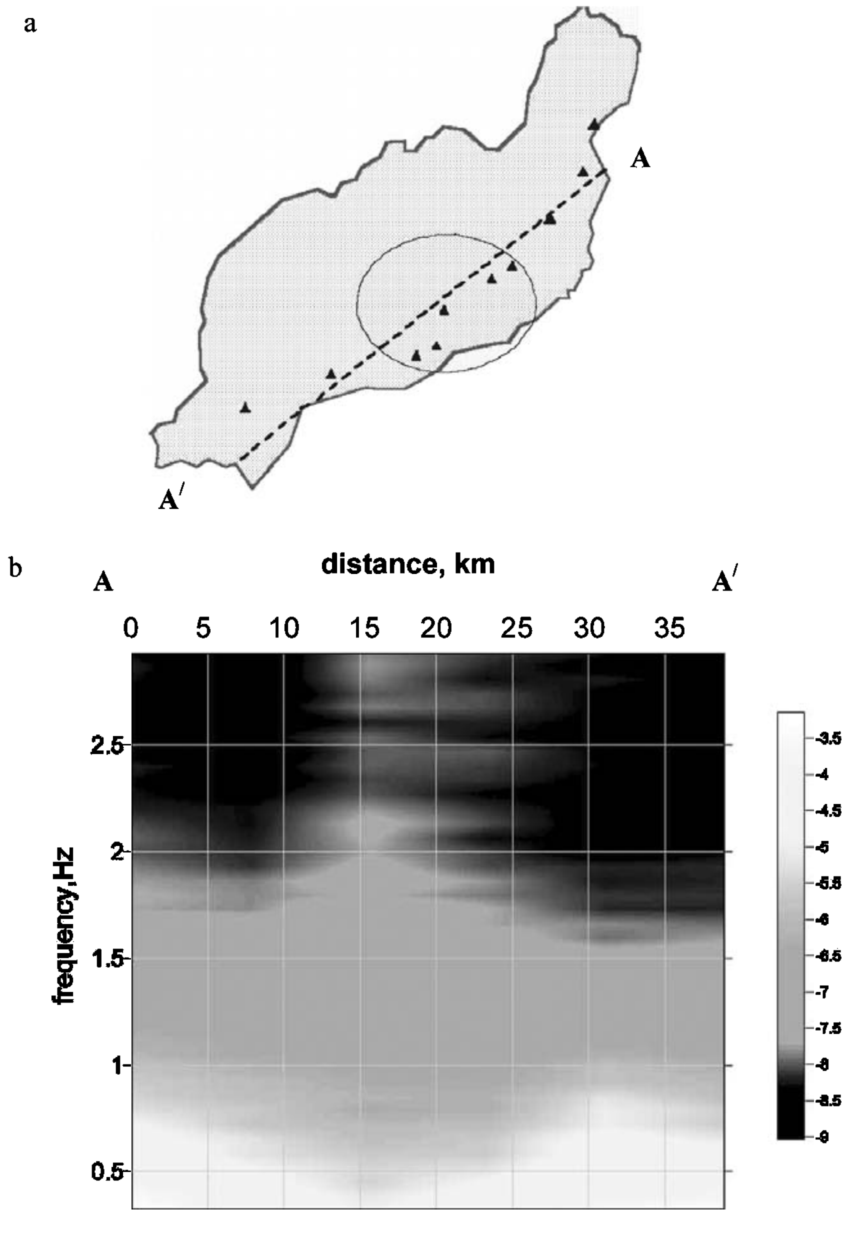

Figure 5
(a) The observational sites, positions in the profile during the summer 2001 campaign. The ellipse with increased density indicates the anomalous zone revealed in summer 2000 campaign. (b) Distribution of stacked spectra amplitudes versus frequency and site position in the profile. Inking indicates the logarithmic amplitudes of microseisms.

one. In the zone where we observed a depression we see amplitude growth. Here we just note this interesting fact. It is probably also in connection with peculiarities of the subsurface geological structure at the given place of the island. However we will not consider and analyze the phenomenon models in this paper.

6. Discussion

In spite of the possibility to explain the observed loss in amplitudes aided by the presence of subsurface rigid inclusion, we made our best effort to attract independent data on other geophysical fields for the same territory.

Thus recently CAMACHO *et al*., (2001) presented results of modelling the crust of anomalous masses of Lanzarote Island, which were based on application of a new version for inverse gravimetry problem solution and data which were obtained in a detailed gravimetry survey of the island in 1988. Figure 6a was adopted from the paper and contains a map of the Bouguer gravimetric anomalies distribution. Dots indicate a network of gravity stations (totally 296 stations). A bright positive anomaly in the center of the island rises above the background near San-Bartolome. The transversal size of this zone is about 13 km. Its mass anomaly constitutes $582*10^{12}$ kg. CAMACHO *et al*. (2001) interpret this anomalous zone as an intrusive body, reaching with its roots to a depth of 15 km, where it almost achieves the Moho boundary alleged here. Up to him the depth of the intrusion is still under discussion. According to MACFARLANE and RIDLEY (1969) this body corresponds to a major igneous center within the crust, it was important at least during the early sub-aerial growth of the island, and may be formed initially at the intersections of fundamental NNE- and SW- trending fault systems. However, while large earth movements and an erosion process may have disrupted this structure until now, only the ridges remain as horst blocks, the central cone having subsided between them and having been covered by younger volcanic eruptions. Moreover, the detailed survey of the island revealed a number of smaller and shallower positive bodies, interpreted as less-developed magmatic intrusions. Unfortunately density of our microseismic network made if impossible for us to distinguish these minor structures, though we can expect to distinguish them in the microseismic field as well if the experiment is properly arranged.

Comparing Figure 4 with Figure 6a we note a remarkable coincidence of anomalous zones revealed in the microseismic and gravimetrical fields. The interpretations of both anomalies independently imply the analogous reason of their formation and namely the presence of an intrusive body in the area of San-Bartolme. We consider this fact a ponderable mutual proof of these interpretations.

Based on the inverse gravimetry problem solution CAMACHO *et al*. (2001) estimated density of the intrusive body. We also endeavored to estimate elastic parameters of this body based on the microseisms amplitudes distribution

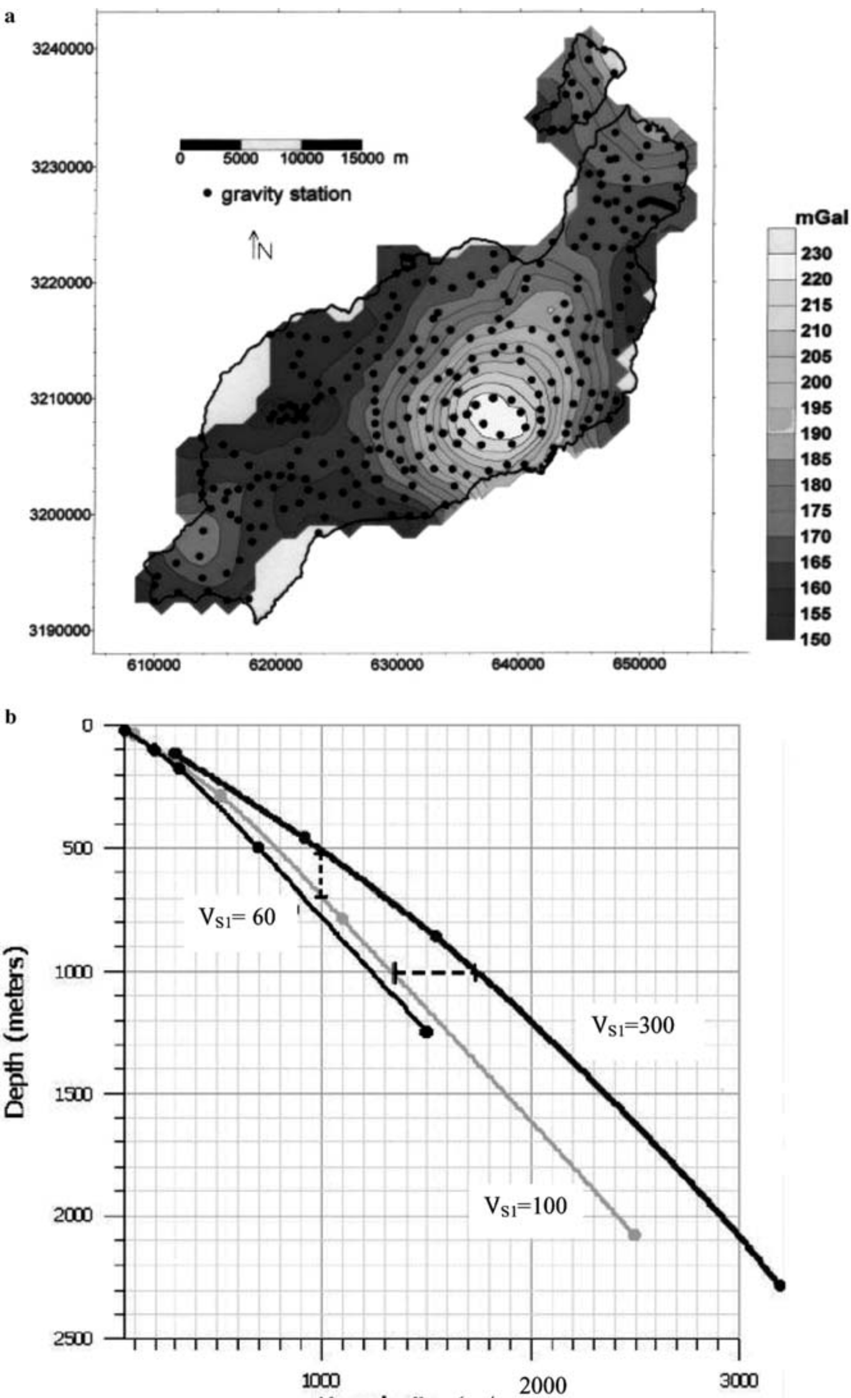
a
3240000
3230000
3220000
3210000
3200000
3190000
610000
620000
630000
640000
650000
0 5000 10000 15000 m
gravity station
N
mGal
230
220
215
210
205
200
195
190
185
180
175
170
165
160
155
150
b
0
500
1000
1500
2000
2500
Depth (meters)
1000
2000
3000
Vs velocity (m/s)
VS1= 60
VS1=300
VS1=100

information. For this we employed a simple elastic model of two half spaces with different values of densities and elastic parameters. According to LEVSHIN *et al.* (1992), a dependence on the depth of Rayleigh wave amplitudes in the half space can be described as follows:

$$A_Z(\omega, Z) = \frac{k^2 - 2}{k^2}\left(e^{-r_\alpha Z} + \frac{2}{k^2 - 2}e^{-r_\beta Z}\right) \ , \tag{2}$$

where

$$r_\alpha = \frac{2\pi}{l}\sqrt{1 - \gamma^2 k^2}; \quad k = V_R/V_S$$

$$r_\beta = \frac{2\pi}{l}\sqrt{1 - k^2}; \quad \gamma = V_S/V_P \quad l - \text{Rayleigh wave length} \ .$$

Making flexible assumptions about retaining the energy when the Rayleigh wave is crossing the vertical boundary, we calculated a relation of amplitudes in waves for the surface in both half spaces based on equation (2). We varied parameters V_S, V_P and V_R for both half spaces trying to approach the calculated result to the experimental amplitude's relations for the anomalous zone and surrounding space of different frequencies. At that we kept the relations between V_S, V_P and V_R within the definite limits existing for the real velocities. We found during the modelling that the amplitude distribution is most sensible to the V_S parameter.

In our calculations we proceeded from values in surrounding space $V_{S1} = 100$ m/s and $V_{S1} = 300$ m/s and estimated the values of V_{S2} and V_{R2} for the anomalous zone. Then we calculated a length of the Rayleigh wave in the anomalous zone and estimated its penetration to the depth using the relation: $H = 1/2\ l$. Results of our estimations are presented in Figure 6b. This figure indicates the distribution of velocities in the intrusive body when approaching the surface. The fragments of the dashed lines illustrate the range of possible velocities for the given depth in one case and the range of depths within which the given velocity can be met in another case. This simple modelling for V_{S2} (shear-waves velocity in the anomalous zone) produced a resulting value typical for basalt (see Fig. 6a.). This is in good agreement with the conclusion of CAMACHO *et al.*, (2001) regarding the existence, position and substance of the intrusive body.

The range of velocities in the surrounding space we chose ($V_{S1} = 100$ m/s and $V_{S1} = 300$ m/s) was not accidental, and was obtained as a result of two

◀

Figure 6
(a) Distribution of gravity stations and the map of the Bouguer gravimetric anomaly. The value used for density of terrain correction is 2,480 kg/m^3 (adopted from CAMACHO *et al.*, 2001). (b) Results of simulation of the distribution of V_{S2} velocity versus depth for the different V_{S1} in the revealed anomalous zone. The V_{S1} magnitudes (given in m/s) accepted for calculations is shown near each curve.

experiments. The first one was described earlier and consisted of the estimation of V_{S1} velocity beyond the anomalous zone from the Rayleigh amplitudes comparison between the surface site and the deepened site in the lava tunnel. It produced the result $V_{S1} = 100$ m/s. The second experiment consisted of direct measurements of velocities of microseisms (beyond the anomalous zone as well). This was done with the help of a small aperture seismic array and resulted in $V_{S1} = 300$ m/s.

7. Conclusions

We performed a microseismic survey at the territory of the Lanzarote Island, Canary Archipelago. For this we used a three-component seismometer which we moved from one site to another. The initial target consisted of searching for the appropriate place to organize the long-term seismic station. We used a velocimeter–type channels with the band 0.3–12.5 Hz for our measurements. Later on a data analysis showed that the microseism's parameters stably depend on peculiarities of the subsurface geological structure.

To interpret correctly the survey data we studied the properties of the microseisms signal. First, we ascertained that microseisms on the island are mainly presented with the surface waves of the Rayleigh-type. It was also illustrated experimentally that frequency-dependent amplitudes decrease with the depth. A microseisms particle motion analysis showed that (for our case at least) the microseisms source has no definite location and looks like a distributed source. Second, we studied a stationarity of microseisms analyzing a standard deviation in increasing the time window and found that after approximately 800 seconds the signal is receiving stationary properties.

During the survey we measured power spectra with 64 times stacking and analyzed a distribution of individual frequency components thereafter for the surface sites. We found that spatial distribution of the spectral components ranging 0.3–1.2 Hz amazingly coincides with the detailed gravity survey data obtained in the independent study. The gravimetric data point to a deep intrusive body in the central part of the island. The microseismic survey results can be explained similarly .

We tried to estimate shear velocities in the surrounding rocks and in the intrusive body as well as the density estimation from gravimetric data. We derived values typical for basalt rocks, which is in agreement with the conclusions of the gravimetric study.

Acknowledgements

We thank Academician V.N. Strakhov, Director of Institute of Physics of the Earth, Russian Academy of Science for organizational support of this research. We are also grateful to the staff of Casa de los Volcanes (Lanzarote) for their assistance. The Contract between the Russian Academy of Sciences and the Spanish Council for Scientific Research has supported this research.

References

Aki, K. (1957), *Space and Time Spectra of Stochastic Waves with Special Reference to Microtremors*, Bull. Earthquake Res. Inst. Tokyo Univ. *35*, 415–457.

Arnoso, J., Fernandez, J., and Vieira, R. (2001), *Interpretation of Tidal Gravity Anomalies in Lanzarote, Canary Islands*, J. Geody. *31*(4), 341–354.

Asten, M. (1978), *Geological Control on the Three-component Spectra of Rayleigh-wave Microseisms*, *Bull. Seismol. Soc.* Am. *68*(5), 1623–1636.

Banda, E., Danobeitia, J. J., Surinach, E., and Ansorge, J. (1981), *Features of Crustal Structure under Canary Islands*, Earth Planet. Sci. Lett., *55*, 11–24.

Bard, P. (1999), *Microtremor Measurements: A Tool for the Effect Estimation*? The Effects of Surface Geology on Seismic Motion, (Balkeman, Rotterdam), 1999 ISBN 90 5809 030 2.

Bendat, J. S., and Piersol, A. G. (1966)*, Random Data: Analysis and Measurement Procedures*, (Wiley-Interscience), New York, 463 pp.

Camacho, A. G., Montesinos, F. G., Vieira, R., and Arnoso, J. (2001), *Modeling of Crustal Anomalies of Lanzarote (Canary Islands) in Light of Gravity Data*, Geophys. J. Int. *147*, 1–22.

Chavez-Garcia, F. J., Cuenca, J., and Lermo, J. (1995), *Seismic microzonation in Mexico. The examples of Mexico City, Oaxaca and Puebla, Proc. 5th Int. Conf. on Seism. Zonation*, Nice, France,. vol**.** **I,** 699–706.

Field, E. H., Hough, S. E., and Jacob, K. H. (1990), *Using Microtremors to Assess Potential Earthquake Site Response: A Case Study in Flushing Meadows, New York City*, Bull. Seismol. Soc. Am. *80*, 1456–1480.

Gorbatikov, A. V. and Barabanov, V. L. (1994), *Experience in Use of Microseisms to Evaluate the State of the Upper Crust*, Phys. Solid Earth, Eng. Transl. *29*(7), 640–644.

Gutenberg, B.,. *Grundlagen der Erdbebenkunde*, Velag von Gebruder Borntraeger, Berlin (1927*)*.

Horike, M. (1985), *Inversion of Phase Velocity of Long–period Microtremors to the S-wave Velocity Structure down to the Basement in Urbanized Areas*, J. Phys. Earth *33*, 59–96.

Hough, S. E., Seeber, L., Rovelli, A., Malagnini, L., DeCesare, A., Seveggi, G., and Lerner-Lam, A. (1992), *Ambient Noise and Weak-motion Excitation of Sediment Resonances: Results from the Tiber Valley, Italy*, Bull. Seism. Soc. Am. *82*, 1186–1205.

Irikura, K. and Kawanaka, T. (1980), *Characteristics of Microtremors on Ground with Discontinuous Underground Structure*, Bull. Disas. Prev. Inst. Kyoto Univ., *30-3*, 81–96.

Kagami, H., Okada, S., Shiono, K., Oner, M., Dravinski, M., Mal, A. K. (1986), *Observation of 1 to 5 Second Microtremors and their Application to Earthquake Engineering. Part III. A Two-dimensional Study of Site Effects in S. Fernando Valley*, Bull. Seismol. Soc. Am. *76*, 1801–1812.

Kanai, K. and Tanaka, T. (1954), *Measurement of the Microtremor,* Bull. Earthq. Res. Inst. Tokyo Univ. *32*, 199–209.

Katz, L. J. and Bellon, R. S. (1978), *Microtremor Site Analysis Study at Beatty, Nevada*, Bull. Seismol. Soc. Am. *68*, 757–765.

Lacoss R. T., Kelly, E. J. and Toksoz, M. N. (1969), *Estimation of Seismic Noise Structure Using Arrays*, Geophys. *1*(34), 21–38.

Lermo, J. and Chavez-Garcia, F. J. (1994), *Are Microtremors Useful in Site Response Evaluation*? Bull. Seismol. Soc. Am., *84*(5), 1350–1364.

Levshin, A., Ratnikova, L. and Berger, J. (1992), *Peculiarities of Surface-wave Propagation across Central Eurasia*, Bull. Seismol. Soc. Am. *82*, 2464–2493.

MacFarlane, D. J. and Ridley, W. I. (1969), *An interpretation of Gravity Data for Lanzarote, Canary Islands*, Earth Planet. Sci. Lett. *6*, 431–436.

MATSUSHIMA, T. and OKADA, H. (1990), *Determination of Deep Geological Structures under Urban Areas Using Long-Period Microtremors*, Butsuri-Tansa, *43*, *1*, 21–33.

NAKAMURA, Y. (1989), *A method for Dynamic Characteristics Estimation of Surface Using Microtremor on the Ground Surface*, QR of RTRI *30*(1), February, 25–33.

OHTA, Y., KAGAMI, H., GOTO, N. and KUDO, K. (1978), *Obsevation of 1 to 5 Second Microtremors and their Application to Earthquake Engineering. Part I: Comparison with Long- period Accelerations at the Tokachi-Oki Earthquake of 1968*, Bull. Seismol. Soc. Am. *68*, 767–779.

OMORI, F. (1908), *On Microtremors,* Res. Imp. Earthquake Inv. Comm. *2*, 1–6.

OMOTE, S. and NAKAJIMA, N. (1973), *Some Considerations for the Relation between Microtremors and Underground Structure*, Bull. Int. Inst. Seism. Earthq Eng. *11*, 9–19.

SAKAJIRI, N. (1982), *Experimental Study on Fundamental Characteristics of Long-period Microtremors*, Bull. H.I.T. *2*, 112–154.

SATO, T., KAWASE, H., MATSUI, M. and KATAOKI, S. (1991), *Array measurements of high frequency microtremors for underground structure estimation. In Proc. 4th. Conf. n Seismic Zonation,*. Stanford, California, vol. *II*, 409–415.

SEO, K., HAILE, M., KURITA, K., YAMAZAKI, K. and NAKAMURA, A., *Study of Site Effect in Kobe Area Using Microtremors,* X-th World Conf. on *Earthquake Engineering*, Acapulco, #1656, (Elselvier Science Ltd).(1996)

UDWADIA, F. E. and TRIFUNAC, M. D. (1973), *Comparison of Earthquake and Microtremor Ground Motions in El Centro, California*, Bull. Seismol. Soc. Am. *63*, 1227–1253.

VIEIRA, R., VAN RUYMBEKE, M., ARNOSO, J. and TORO, C. (1991), *The Lanzarote Underground Laboratory*, Cahiers du Centre Europeen Geodynamique de Seismologie *4*, 71–86.

(Received February 15, 2002, revised December 23, 2002, accepted January 29, 2003)